Spectrochimica Acta Part A: Molecular and Biomolecular Spectroscopy 330 (2025) 125675

Contents lists available at ScienceDirect

Spectrochimica Acta Part A:
Molecular and Biomolecular Spectroscopy

journal homepage: www.journals.elsevier.com/spectrochimica-acta-part-a-molecular-and-biomolecular-spectroscopy

Application of FTIR spectroscopy to infer ante- and post-mortem changes in archaeological human bone

Marta Colmenares-Prado [a,*], Antonio Martínez Cortizas [a,d], Clara Veiga-Rilo [b], Olalla López-Costas [b,c]

[a] CRETUS, EcoPast (GI-1553), Facultade de Bioloxía, Universidade de Santiago de Compostela, 15782 Santiago de Compostela, Spain
[b] Group EcoPast (GI-1553), CRETUS, Area of Archaeology, Dpt of History, Universidade de Santiago de Compostela, Santiago de Compostela, 15782, Spain
[c] Archaeological Research Laboratory, Stockholm University, Wallenberglaboratoriet, SE-10691 Stockholm, Sweden
[d] Bolin Centre for Climate Research, Stockholm University, 10691 Stockholm, Sweden

HIGHLIGHTS

- Post-Roman human bones (ribs, long bones, crania) from A Lanzada were analysed by FTIR.
- The MIR indices and the study of the whole spectra (by PCA) give new insights into ante- and post-mortem alteration of bone.
- Ribs were more altered than cranial bones.
- Chemical composition of bones was influenced not only by the post-mortem processes but also the ante-mortem conditions.
- The widely used Am/P index may be not as useful for the assessment of diagenesis degree in bone as previously conceived.

GRAPHICAL ABSTRACT

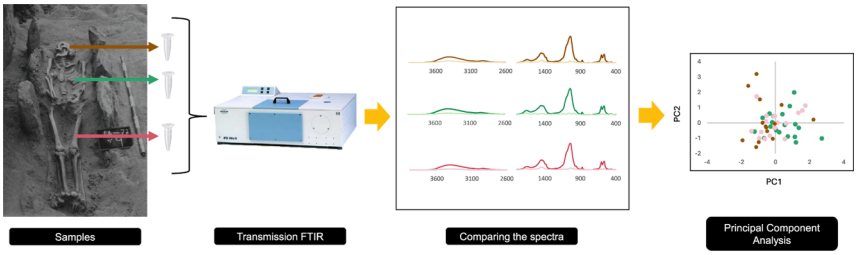

ARTICLE INFO

Keywords:
FTIR
Ante-mortem
Diagenesis
Bone type
Age-at-death

ABSTRACT

Several studies have used Fourier Transform Infrared Spectroscopy (FTIR) to assess chemical and structural changes caused by diagenesis in archaeological human bone, whereas other factors such as individual's biological profile (sex and age) or the type of bone have seldom been considered. In this study transmission FTIR was applied to 51 bone samples from 19 post-Roman individuals of A Lanzada necropolis (NW Spain). Mid-infrared (MIR) indices (IRSF, MMI, C/P, C/C, Am/P, BPI, API, AmI/AmII) were also calculated and principal component analysis (PCA) was used to explore peak ratios and differences across the whole spectrum. PCA components showed correlation to the C/P and Am/P indices, as well as differences in the Amide III absorbance trends versus Amide A, B, I and II. Signals related to soil material (silicates and aliphatic organic matter) were also revealed by the PCA in some samples. No significant differences in bone composition per sex were found, but cranial carbonate content was significantly higher in non-adults than in adults, and ribs presented a higher amide-to-phosphate ratio (Am/P) than femora and crania. Ribs showed the most altered bioapatite, in agreement with a previous study based on the elemental composition of the samples analysed here. Bioapatite alteration may be

* Corresponding author.
E-mail addresses: marta.colmenares@usc.es (M. Colmenares-Prado), antonio.martinez.cortizas@usc.es (A. Martínez Cortizas), clara.veiga.rilo@usc.es (C. Veiga-Rilo), olalla.lopez@usc.es (O. López-Costas).

https://doi.org/10.1016/j.saa.2024.125675
Received 30 July 2024; Received in revised form 24 December 2024; Accepted 26 December 2024
Available online 27 December 2024

responsible for the higher amide content relative to phosphate (i.e., preferential preservation of collagen) in ribs. Thus, caution is advisable when using the Am/P index to assess collagen preservation.

1. Introduction

The preserved materiality of human bodies through time is usually composed of bones and teeth, i.e., skeletons. Many of those skeletons were inhumated and bone composition after the exhumation is the result of the combination of bone ante-mortem composition with bone post-mortem modifications, mainly related to soil-body interaction. Bone is a biological tissue, characteristic of vertebrates, formed by a mineral phase, bioapatite, consisting of carbonated hydroxyapatite crystals ($Ca_{10}(PO_4)_6(OH)_2$) (approximately 60 % of total weight), an organic matrix mainly composed by type I collagen, non-collagenous proteins and lipids (approximately 30 % of the total weight), and water (around 10 % of bone weight) (among many others [1–4]). Diagenesis, when referred to human remains, encompasses the chemical, physical, mineralogical, and histological changes in the skeleton due to their interaction with the soil [5,6]. Hedges [7] proposed that bone diagenesis implies collagen loss, and mineral transformations (i.e., increase in crystallinity and dissolution and uptake of ions), which are mainly determined by the hydrology of the site [4]. Chemical degradation of collagen is influenced by a variety of factors. The most important ones are temperature (the higher the temperature, the more the collagen decays), soil acidity/alkalinity (highly acidic and highly alkaline soils favour collagen degradation), the presence of cracks by the action of weathering or gnawing (that leave the bone more exposed to external agents), and presence of water (increase in collagen loss) [8,9]. For bioapatite, diagenetic change results in an increase in crystallinity and apatite recrystallization (i.e., increase in crystal length and lattice order, as well as changes in crystal shape) [10]. Recrystallization is, in part, triggered by collagen loss, since the crystals get more exposed to water and ion incorporation [7,8], during the earliest diagenetic stages [11]. These changes are also influenced by soil acidity/alkalinity. Between pH between 7–9 bioapatite is more stable, and therefore less prone to dissolution [8,12]. The degradation of the organic matrix of the bone and the alteration of the mineral lattice are highly related. Whether it is the collagen that prevents the dissolution of the bioapatite, or the dissolution of bioapatite that triggers collagen degradation by leaving it exposed to microorganism action is still debated, and it seems to depend on the conditions of the burial environment [10].

Human skeletons are studied from different approaches – archaeology, biological anthropology, medicine, etc. Archaeology aims to distinguish both – ante- and post-mortem phases – to reconstruct ante-mortem features of bone and link them with the lifestyle conditions of the individual, and the socio-cultural background. Biological anthropology aims to better understand the human species, especially focusing on post-natal growth and features determined by the biological profile (i.e., sex, age, population background). Medical disciplines aim to obtain information about the human skeleton physiology and histology by performing invasive analyses (not feasible in vivo) and cover a greater number of life conditions. In all cases, studies are focussed on skeletons from archaeological and/or forensic contexts. The analysis of archaeological bones often involve destructive biogeochemical analyses (e.g., DNA, stable isotopes, proteomics studies). It is of paramount importance to promote methods that minimize the destruction of the skeletons to preserve our cultural heritage, and still allow the study of bone development during growth, renewing processes, and remodelling. Fourier transformed infrared (FTIR) spectroscopy is one such technique to characterize of the organic and inorganic molecular structure of a wide range of materials (in liquid or solid state) by measuring the vibrational modes of the molecules within the material in response to mid-IR radiation [13]. This technique is also a powerful tool for evaluating the composition of archaeological materials, including human bone. Mid infrared FTIR covers a wavelength range (4000 and 400 cm^{-1}) that makes it ideal to trace molecular features and diagenesis of both collagen and bioapatite. Molecular changes in collagen composition can be detected by variations in the absorbance of the amide A and B region (3600–3200, ~3070 cm^{-1}), the amide I, II, and III regions (1650–1600, 1550–1500, 1310–1175 cm^{-1}), as well as the presence of aliphatic compounds (~2930, ~2850 cm^{-1}). Changes in bioapatite content and structure can be traced, for example, by variations in carbonate substitutions (1450–1400 cm^{-1}), and crystallinity (~600, ~557 cm^{-1}) [14–19]. ATR-FTIR has now become the predominant infrared spectroscopy technique in archaeological studies, because of the fast and easy nature of sample preparation and that it is as reliable as transmission FTIR [9,14,18]. However, transmission FTIR with KBr pellets was the technique of choice in the present study since it allows a more reliable replication of the measures – the pellets are re-measurable, when compared with ATR-FTIR in which the surface of the sample is different every time that is measured. In addition, transmission FTIR only needs a small amount of sample, and the sample can be recovered by diluting the exogenous components.

During the last decade, applications of FTIR spectroscopy in the study of human bone had largely increased. This technique has been employed with medical purposes, such as detecting pathogens in bone grafts (e.g., [20]), characterise bone repair after surgery (e.g., [21]) or for pathology diagnosis (e.g., [22]). Also, it has been tested in forensics as a tool for post-mortem interval estimation (e.g., [23]). In archaeology, FTIR has been used in several studies to address bone diagenesis (e.g., [9,24–26]). Many of them apply FTIR as a quick prior to or as a subsequent step to destructive analyses, such as those employed in paleogenetics, paleodiet, or paleomobility [27,28]. Others tried to establish a relationship between sex or age-at-death and diagenesis [3,4,24–26,29] as well as type of bone and degree of diagenesis [9,25,29–33] to improve our understanding of diagenetic patterns between bone types in order to select the most suitable bone before performing destructive analyses [9,25]. New perspectives include the study of decaying patterns in adult and non-adult individuals [24], or the prediction of long-term preservation of bone [34]. Those studies mainly calculate MIR indices to assess bone crystallinity, collagen content relative to phosphate, and the ratio of carbonate-to-phosphate. They do not consider the full spectrum, and they focus only on specific absorbance regions, losing valuable information on the molecular features and diagenesis of the bones (with some exceptions, [2,25,35,36]).

Although diagenesis has been widely studied, the ante-mortem characteristics of bone have been largely ignored, despite being crucial to understanding bone degradation processes but also aspects of bone growth, turnover, and physiological alterations. Although some medical studies of fresh bone were performed on this issue (e.g., [37–39]). Thus, FTIR spectroscopy has been used to understand post-mortem alterations, without considering the fact that the starting point for diagenetic changes may be different among individuals or even for different bones within the same skeleton. In the present study, we aim to assess the role of ante-mortem features such as biological profile (i.e., age and sex) and bone type on bone composition as well as diagenetic alteration. To this end, we analysed by transmission FTIR a collection of archaeological skeletons of different age-at-death and sex, considering three types of bone (ribs, long bones, and crania) that present different formation patterns and turnover rates. The skeletons were buried for a sufficient length of time (~1,500 years) for soil-induced changes to take place, but not too old to expect fossilization. For the selected collection (A Lanzada post-Roman individuals), paleodiet and diagenesis (from an elemental composition perspective) were previously studied [40,41]. Combined with FTIR, these data are key to try to

differentiate the ante-mortem from the post-mortem processes. In the present study, FTIR was combined with multivariate analysis of the spectrum together with the analysis of the well-established MIR indices applied in diagenesis studies during the last few years to prove how these two perspectives can provide a more integrated knowledge of the molecular profile of the samples.

2. Material and methods

2.1. Archaeological context and sample collection

Human bones from A Lanzada (Noalla, Sanxenxo; Pontevedra) archaeological site (Fig. 1) were analysed. The site contains archaeological remains dated from the Bronze Age to Medieval times [42–48]. The most relevant finding for this study is a large necropolis with two funerary areas. One was dated in Roman times (AD 1st–4th centuries) and is located at the North side of the site [42,43,49]. This area was excavated during the 1940s and 1950s, with a deficient recovery of skeletons (no non-adult skeletons or short bones were recovered), so the skeletal assemblage is comprised of adult crania and long bones. Information about the burial typology of all skeletons is also poor. A post-Roman funerary area (AD 4th–7th centuries) located South, that was excavated during the 1970s and in 2016 [44,45,49]. Despite the lack of archaeological reports, photographs taken during the 1970s campaigns provided detailed archaeological information. A detailed description of these funerary areas and additional information about radiocarbon dating can be found elsewhere [49–51].

Samples of finely milled cortical bone belonging to individuals of the post-Roman (AD 4th–7th centuries) funerary area were analysed. Since samples were obtained from previous studies [40,52] and transmission FTIR is non-destructive, we consider that the present study meets the ethical standards for analysing archaeological bone, given that the questions proposed here cannot be solved without employing chemical analyses that require sampling [53]. A total of 51 samples from 19 individuals were studied: 6 males (15 samples), 6 females (17 samples), and 7 non adults (19 samples). The age profile (following Vallois classification [54]) comprised 8 young adults (20–39 years), 3 middle adults (39–60 years), 1 old adult (>60 years), 3 juveniles (12–19 years), 3 children (4–11 years) and 1 infant (<3 years). For every individual, three bone types were analysed: thoracic (19, mainly ribs but also vertebrae when rib was not available), crania (14, including mandible), and long bones (18, mainly femur, but also humerus when femur was not available) (see Supplementary Table 1.) Published data previous investigations on the same skeletons or skeletons from the same site, were also used [40,41,49,51,52,55,56].

2.2. Methods

Transmission FTIR spectroscopy was performed at the IR-RAMAN unit of RIAIDT (Universidade de Santiago de Compostela, Spain) using a Bruker IFS-66 V FTIR spectrometer. One milligram of homogenized (milled) raw sample was mixed thoroughly with 100 mg of KBr (FTIR grade) and a pellet was prepared using a press. Pellets were prepared by the same person, an (she) IR-expert of the RIAIDT unit, during the same month to minimize possible bias related to sample preparation. Spectral resolution was set to 4 cm^{-1} and 32 scans per sample were recorded in the mid-infrared range (4000–400 cm^{-1}). A background was collected before analysing every sample. To avoid differences in absorbance

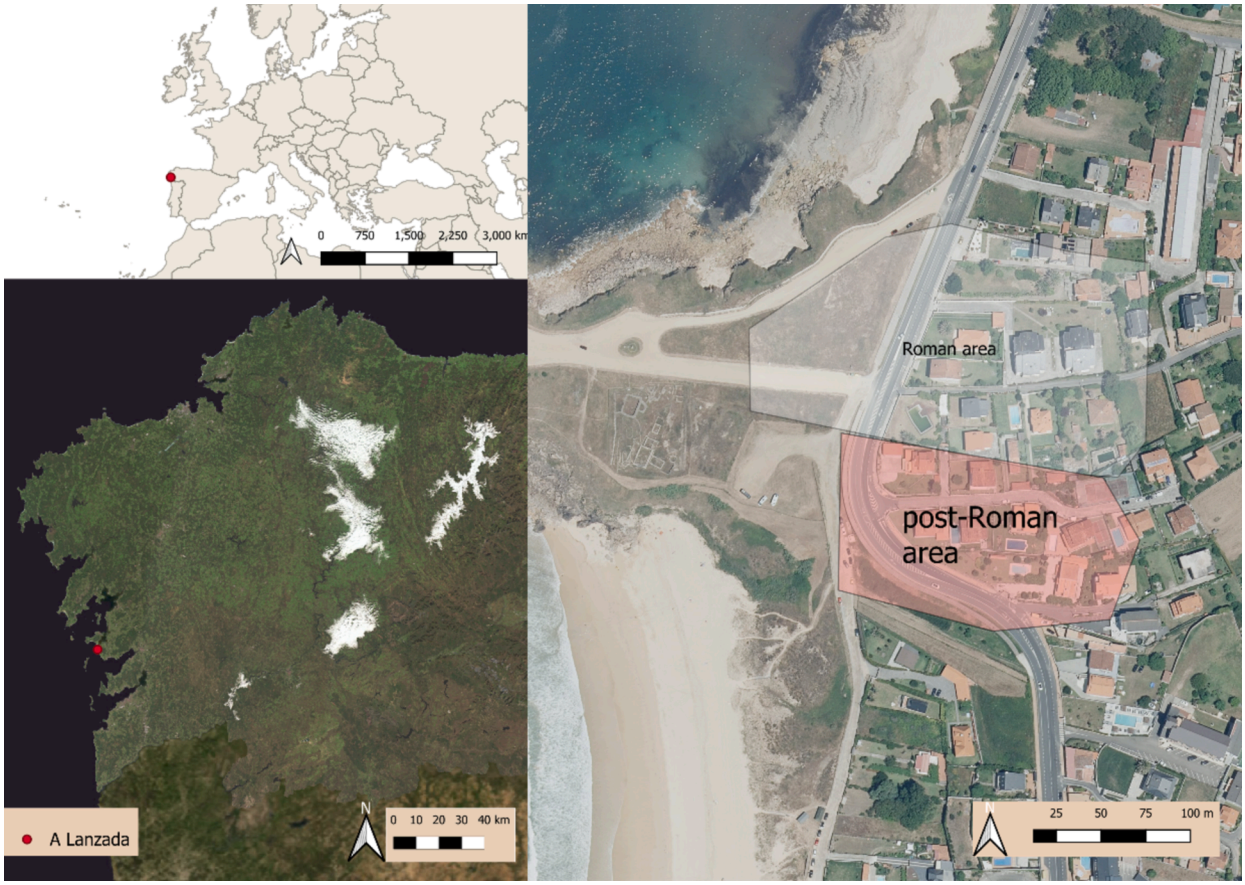

Fig. 1. A Lanzada and its location in Europe (A), Galicia (B) and an aerial view of the site (C), with the Roman and post-Roman areas of the necropolis highlighted in white and red, respectively. (A) is a modified template from QGIS.38.2, and (B) and (C) were modified from Plan Nacional de Ortofotografía Aérea (PNOA) map from Instituto Geográfico Nacional.

related to sample preparation and detection, the R routine {*andurinha*} [57] was applied to normalize the spectra and make them comparable. Second derivative spectra were also obtained with {*andurinha*} and used to locate the main absorbances/peaks (i.e., wavenumber) of all the samples. Peak assignment to the different functionalities was done based on literature [15,16,56,58–61]. Baseline correction, using the R package *{baseline}* [62], was applied to the whole spectrum (from 4000 to 400 cm^{-1}), so the distortions caused by optical scattering effects are amended [63]. The following MIR indices that are frequently used in bone research to assess bone composition and structural changes were also calculated:

- Infrared Splitting Factor, IRSF (604 + 563)/590 cm^{-1}), following France et al. [17] recommendations for raw samples. This index indicates the crystallization degree of bone bioapatite, that means, the size/strain [64].
- Mineral Maturity Index, MMI (1034/1105 cm^{-1}), which is related to the transformation of the non-apatitic domains into apatitic domains [65].
- Ratio between $\nu_3(CO_3^{2-})$ and $\nu_1\nu_3(PO_4^{3-})$, C/P (1420/1034 cm^{-1}) [58] $\nu_3(CO_3^{2-})$ was selected for the measurement of the carbonate-to-phosphate ratio since this vibration mode is clearly separated from the main phosphate bands [58].
- Ratio of B-type carbonates to phosphates, BPI (1420/604 cm^{-1}) [17], related to the extent of carbonate substituting for phosphate
- Ratio of A-type carbonate-to-phosphate, API (1540/604 cm^{-1}) [17], related to the extent of carbonate substituting for hydroxyl.
- A-type carbonate to B-type carbonate ratio, C/C, (1452/1420 cm^{-1}) [17], to assess the relative dominance of carbonate substitution.
- Amide I/phosphate ratio, Am/P (1638/1034 cm^{-1}), which indicates the collagen/mineral content of bone [66].
- Amide I to Amide II ratio, AmI/AmII (1663/1549 cm^{-1}), to trace collagen denaturalization [67].

All indices were calculated using maximum peak absorbance intensity of the selected bands. Recommendations on analytical quality proposed by Smith et al. [63] for the study of bone diagenesis by FTIR spectroscopy were applied. The symbol ν refers to vibrational modes ((ν_1 = symmetric stretching, ν_2 = symmetric bending, ν_3 = asymmetric stretching, ν_4 = asymmetric bending) [68]. We use this nomenclature because it is widely used in vibrational spectroscopy of archaeological bone.

2.3. Statistical analyses

Principal Component Analysis (PCA) was performed by applying varimax rotation on correlation mode. For statistical comparison between groups of samples (i.e., bone type, sex, age-at-death) and due to the relatively small sample size of the groups, a non-parametric Mann-Whitney *U* test (α = 0.05) was performed. The test was applied to the IR variables (principal components and MIR indices) to check for significant differences. Since 3 types of bone were taken from each individual, when possible, the data were analysed separately in order to avoid overrepresentation. For correlation analysis, the Spearman correlation coefficient was performed as some variables do not follow a normal distribution. Correlation was also performed between data obtained in this study and that obtained in previously [41] as well as between the Am/P index and collagen quality and quantification parameters. PCA, Mann-Whitney *U* test and correlation analysis were executed using IBM SPSS Statistics 29 Software.

3. Results

Large absorbance is observed in the 1150–970 cm^{-1} region, $\nu_3(PO_4^{3-})$ asymmetric stretching, which is the main absorbance band of phosphate from the bioapatite (Table 1; Fig. 2). Moderate absorbance is observed in the regions between 3600–3200 cm^{-1} (Amide A: that is, NH stretching), 1700–1600 cm^{-1} (Amide I: C=O stretching), 1500–1400 cm^{-1} ($\nu_3CO_3^{2-}$, main absorbance of carbonate), and 604 together with 563 cm^{-1} (the $\nu_4(PO_4^{3-})$ doublet which corresponds mainly to bending vibrations). Low absorbance is also shown between 3130–3010 cm^{-1} (Amide B: NH stretching), 3000–2831 cm^{-1} (CH_2 stretching, mainly attributed to aliphatic compounds), as well as the bands at 961 cm^{-1} (symmetric stretching of $\nu_1(PO_4^{3-})$), 876 cm^{-1} ($\nu_2CO_3^{2-}$ bending), and 471 cm^{-1} (attributed to phosphate [59]). In addition, some of the samples presented bands at 3697 and 3622 cm^{-1} (clay), 1597–1514 cm^{-1} (Amide II, CH stretching and NH bending), 1317 cm^{-1}, 1283, 1236 and 1204 cm^{-1} (Amide III: CN stretching and NH bending), 1165, 799, 777 and 694 cm^{-1} (quartz), as it can be seen in Fig. 2-A. A summary of the absorbance regions and band assignment can be found in Table 1. The second derivative spectrum (Fig. 2-C) enabled the identification of phosphates (1034, 961, 604, 563 and 471 cm^{-1}), carbonates (1452, 1420, 876 cm^{-1}), amides (3427, 3061, 1663, 1638 cm^{-1}), aliphatic compounds (2926 cm^{-1}), as well as quartz (799, 777, 694 cm^{-1}) and clay (3697, 3622, 669 cm^{-1}).

Table 1
Main absorbance bands from bone and their assignation to bone compounds.

WN (cm^{-1})	Vibrational mode	Comments	References
3600–3200	NH st + OH st	Amide A + OH	[15,16,56,59]
3130–3010	NH st	Amide B	[15,16]
3000–2831	CH_2 st	Aliphatics	[15,16,59]
1700–1600	C = O st	Amide I	[15,16,56,59–61]
1597–1514	CH st NH bd	Amide II	[15,16,59–61]
1500–1400	CO_3^{2-} asym st+ CH_2 wg + bd	Carbonate + organic	[16,58,59,61]
1320–1200	CN st NH bd	Amide III	[15,16,56,59–61]
1150–970	(PO_4^{3-}) asym st	Phosphate	[15,58,59–61]
961	(PO_4^{3-}) sym st	Phosphate	[15,59–61]
876	(CO_3^{2-}) sym bd	Carbonate	[15,58,59–61]
604	(PO_4^{3-}) asym bd	Phosphate doublet	[15,56,59–61]
563	(PO_4^{3-}) asym bd	Phosphate doublet	[15,56,59–61]
471	(PO_4^{3-}) sym bd	Phosphate	[59–61]

Referred to vibration types = St: stretching (sym: symmetric, asym: asymmetric); bd: bending; wg: wagging.

The standard deviation spectra (Fig. 2-B) show that the largest variability between samples occurs in the amide A (3600–3200 cm^{-1}), Amide I (1690–1640 cm^{-1}), carbonate (1470–1420 cm^{-1}), and 1180–1100 cm^{-1} ($\nu_3(PO_4^{3-})$) regions, as well as the peaks at 1034 cm^{-1} $\nu_3(PO_4^{3-})$, the 997 cm^{-1} ($\nu_3(PO_4^{3-})$), the 604–563 cm^{-1} doublet $\nu_4(PO_4^{3-})$ and 471 cm^{-1} (phosphate – some silicates also absorb in this region). The maximum intensity at 1030 cm^{-1} ($\nu_3(PO_4^{3-})$) indicates a high degree of maturation of the apatite i.e., a well-crystallized mineral bioapatite [69] Despite the overall similarity, there is some variation between the bone types. Ribs show higher variation at Amide I, II and III regions. Long bones have the lowest variation between samples, except for the carbonate region (1500–1400 cm^{-1}). Cranium samples show the highest variation at 3600–3150 (Amide A, OH), 1497–1398 ($\nu_2CO_3^{2-}$), 1069–991($\nu_3(PO_4^{3-})$), 876 (carbonate), 604 and 563 cm^{-1} ($\nu_4(PO_4^{3-})$ doublet).

As for the MIR indices, the obtained results were: IRSF 3.16 ± 0.18 avg ± std; MMI 1.65 ± 0.08; C/P 0.35 ± 0.07; C/C 1.07 ± 0.06; Am/P 0.14 ± 0.05; BPI 1.10 ± 0.27; API 0.43 ± 0.12; AmI/AmII 1.03 ± 0.13 (Fig. 3). As a reference for well-preserved bone we followed the ranges proposed by France et al. [17] for the indices these authors worked with. Values presented here exceed those proposed in [17], but this result must be treated with care since diagenetic changes in bone are site-specific [5,7,25,67]. Furthermore, the ranges proposed by these authors were obtained by ATR-FTIR, and the values for IRSF and C/P have been demonstrated to differ between ATR-FTIR and transmission FTIR [14,18,70]. API was calculated following France et al. [17],

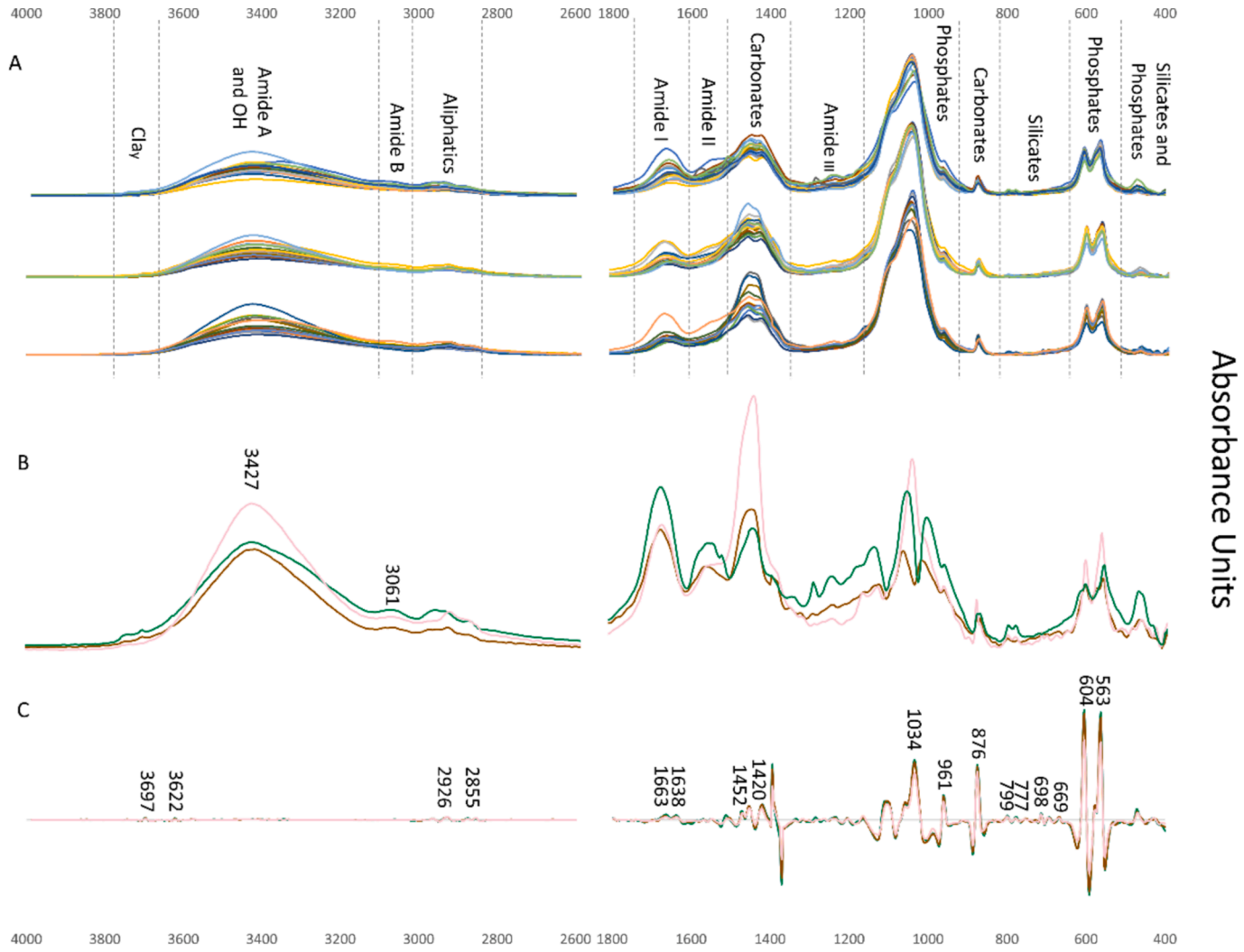

Fig. 2. (A) Normalized spectra for ribs (up), long bones (middle) and cranium (below) from 4000 to 2600 cm^{-1} and 1800 to 400 cm^{-1}. (B) Standard deviation spectra for ribs (green), long bones (brown) and cranium (pink). (C) Second derivative spectra for ribs (green), long bones (brown) and cranium (pink). Second derivative values are reversed to match the absorbance peaks.

nevertheless, this index was not considered in further detail as Amide II from collagen also absorbs at 1540 cm^{-1} and it can mask the A-type carbonate signal.

Principal Component Analysis (PCA) extracted six components (PCs) that accounted for ~94 % of the total variance. Bands associates to each PC and their loadings are shown in Table 2 and in Supplementary Fig. 1. PC1 (31.1 % of the total variance) shows high positive loadings (>0.7) for Amide I (1663, 1638, 1609 cm^{-1}), Amide II (1585, 1568, 1549, 1508 cm^{-1}) and B (3061 cm^{-1}), as well as one band characteristic of aliphatics (2964 cm^{-1}). PC2 (20.0 % of the total variance) presents high positive loadings for carbonates (1472, 1452, 1420, 876 cm^{-1}) and moderate (−0.69 to −0.3) negative loadings for phosphates (1034, 604, 563 cm^{-1}). PC3 (17.1 % of the total variance) shows high and moderate positive loadings for Amide III absorbances (1317, 1283, 1263, 1236, 1204, 1165 cm^{-1}) and moderate positive loadings for phosphate absorbances (1105, 961 cm^{-1}). PC4 (12.8 %) presents high positive loadings for Amide A (3574, 3427, 3341 cm^{-1}). PC5 (9.5 % of the total variance) shows high and moderate positive loadings for aliphatic absorbances (2926, 2874, 2855 cm^{-1}). PC6 (3.4 % of the total variance) shows a high positive loading for the peak at 471 cm^{-1}, attributed to phosphate – but also to silicates. The scores of the principal components are projected in Fig. 4. Rib samples show general positive PC1 scores, and four rib samples show high positive scores for PC3 (240_1, 247_1, 252_1, 271_1). Cranium samples show negative scores for PC3 and PC6, but positive scores for PC5. Whereas long bone samples show general negative scores for PC3, PC4 and PC6, and positive scores for PC5. No patterns were found for PC2.

Mann-Whitney test for bone type showed significant differences ($p < 0.05$) for PC1 between ribs and cranium ($p = 0.004$); for Am/P between ribs and long bones ($p = 0.024$) and ribs and cranium ($p = 0.021$); for API between ribs and cranium ($p = 0.05$); and for C/C between ribs and cranium ($p = <0.001$) and long bones and cranium ($p = 0.003$). Regarding sex as the grouping variable, only ribs from male individuals showed statistically lower PC2 values ($p = 0.041$) than females. As for the age as grouping variable, individuals were grouped into two categories: adults and non-adults. Significant higher values in non-adults when compared with adults were detected for cranium bones for PC2 ($p = 0.019$), C/P ($p = 0.029$), and BPI ($p = 0.019$). On the other hand, significant higher MMI values for adult individuals in cranium bones were detected ($p = 0.042$). As for the Spearman correlation analysis, PC1 is correlated with Am/P ($r_s = 0.778$; $p = <0.001$), while PC2 is correlated with C/P ($r_s = 0.878$; $p = <0.001$), and BPI ($r_s = 0.888$; $p = <0.001$). C/P is correlated with BPI ($r_s = 0.911$; $p = <0.001$), Am/P is correlated with AmI/AmII ($r_s = 0.789$; $p = <0.001$). Furthermore, Am/P index, and PC1 scores of rib samples are correlated with collagen yield values ($r_s = 0.717$, $p = 0.003$, and $r_s = 0.817$, $p = <0.001$, respectively).

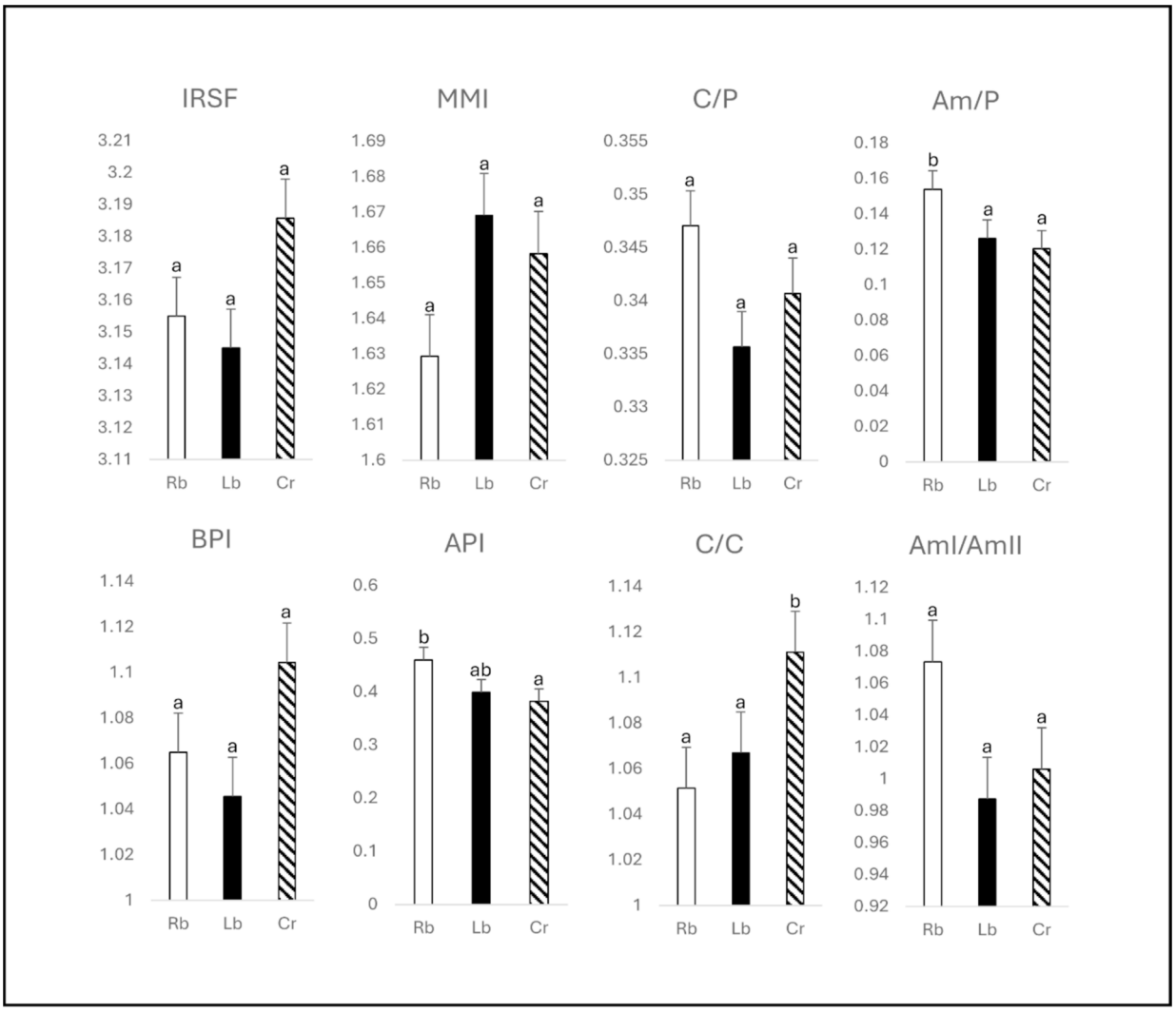

Fig. 3. IR indices (average and standard deviation). Samples are displayed in three different series depending on bone type: rib = Rb; long bone = Lb; cranium = Cr. Letters (a, ab, b) indicate statistical significance, i.e., groups with the same letter showed no statistically significant differences.

Moderate correlations were found between IRSF-C/P (r_s = -0.596; p = <0.001), C/P-Am/P (r_s = 0.607; p = <0.001), PC2-IRSF (r_s = -0.419; p = 0.002) and PC1-AmI/AmII (r_s = 0.500; p = <0.001) (Fig. 5).

4. Discussion

The PCA identified six main FTIR signals related to the bone components' variations: collagen content (PC1), bioapatite carbonate substitution (PC2), Amide III content (PC3), Amide A content (PC4), the content of aliphatics (PC5), and a mixed phosphate/silicate signal (PC6). PCA results are in good agreement with the FTIR indices and, provide additional information (i.e., differences in collagen composition and decay patterns between samples). This is in line with previous studies that recommended the use of multivariate statistical techniques when studying diagenetic processes in skeletal remains [71]. The only index that shows no correlation to the principal components is the IRSF. Below, we discuss the results of the chemometric indices and the PCA in four sections: bone mineral components, bone organic components, differences between bone types, and the relationship to age-at-death and sex.

4.1. Bone mineral components

Average IRSF for our samples is 3.16 ± 0.18 and can be considered low according to Smith et al. [63]. Values are lower than the ones observed by Álvarez-Fernández et al. [56] for the three post-Roman individuals (L01 = 4.3 ± 0.3; L06 = 3.9 ± 0.9; L07 = 4.1 ± 0.5) from A Lanzada site (excavated in 2016). The range of IRSF values (2.86–3.66) also corresponds to values characteristic of well-preserved skeletal tissue according to France et al. [17] although, these authors did not use the same FTIR technique, a fact that can introduce bias. The IRSF values presented here are consistent (or lower, see [25]) with values reported in investigations that used transmission FTIR in archaeological human bones [10,14,18,19,24,72,73].

C/P values (0.35 ± 0.07) are higher than those reported by France et al. [17], based on ATR-FTIR, for well-preserved human archaeological bones, but they fall within the range of results obtained with transmission FTIR both on modern human bone (0.110–0.253; [24,74]), and on archaeological bone (0.18–0.53) [18,19]. Nevertheless, other authors have reported higher C/P (0.4–0.7, [75]) and lower C/P values (0.165–0.302, [74]; 0.04–0.35, [14]; 0.04 ± 0.01, [25]). According to Smith et al. [63], C/P values higher than 0.19 indicate high carbonate content, which is the case for the samples analysed in the present study. However, that differences in C/P regarding modern bones (either higher or lower) are interpreted as diagenetic alteration [14].

In our samples, IRSF is negatively correlated with C/P (r_s = −0.596, p = <0.001), as also reported in previous investigations [9,10,25,26,76,77] It has been suggested that carbonate substitution of

Table 2
Loadings of the principal components and compound assignment.

Compound	Bands	WN (cm^{-1})	PC1	PC2	PC3	PC4	PC5	PC6
	Amide II	1568	**0,950**	0,050	0,239	0,029	0,099	−0,060
	Amide II	1549	**0,947**	0,081	0,278	0,005	0,108	−0,050
	Amide II	1585	**0,925**	0,089	0,185	0,070	0,104	−0,040
Collagen	**Amide I**	1609	**0,917**	0,196	0,150	0,204	0,174	0,049
	Amide I	1663	**0,908**	0,067	0,312	0,168	0,111	−0,010
	Amide I	1638	**0,890**	0,126	0,268	0,259	0,148	0,028
	Amide II	1508	**0,818**	0,433	0,188	−0,040	0,164	0,146
	Amide B	3061	**0,810**	−0,125	0,200	0,179	0,440	−0,010
	Aliphatics	2964	**0,722**	0,084	0,246	0,297	0,557	0,054
	Carbonates	1420	0,214	**0,946**	−0,030	0,140	0,123	0,056
	Carbonates	1452	0,017	**0,939**	−0,010	0,271	0,131	0,033
Carbonate-to-phosphate	**Carbonates**	1472	0,148	**0,926**	0,051	0,253	0,141	0,076
	Carbonates	876	0,216	**0,903**	0,240	0,081	0,058	−0,120
	Phosphate	563	0,552	**−0,620**	0,091	−0,350	−0,105	−0,350
	Phosphate	604	0,423	**−0,634**	−0,170	−0,360	−0,142	−0,400
	Phosphate	1034	−0,200	**−0,658**	−0,300	−0,450	−0,168	−0,050
	Amide III	1165	0,233	0,158	**0,920**	0,174	0,125	0,086
	Amide III	1204	0,396	0,015	**0,888**	−0,010	0,093	0,132
Amide III	**Amide III**	1236	0,553	0,090	**0,757**	0,049	0,218	0,159
	Amide III	1263	0,533	0,226	**0,696**	0,159	0,271	0,100
	Phosphate	961	0,619	−0,321	**0,624**	−0,220	0,067	−0,120
	Phosphate	1105	0,107	−0,395	**0,573**	−0,390	−0,172	0,173
	Amide III	1283	0,514	0,167	**0,559**	0,105	0,256	0,072
	Amide III	1317	0,334	0,453	**0,549**	0,276	0,391	0,053
	Phosphate	1057	−0,516	−0,453	**−0,534**	−0,386	−0,112	0,001
	Amide A – OH	3574	0,303	0,235	0,072	**0,881**	0,212	0,044
Amide A	**Amide A – OH**	3427	−0,017	0,419	−0,010	**0,853**	0,280	0,064
	Amide A – OH	3341	0,189	0,399	0,104	**0,811**	0,343	0,029
	Aliphatics	2855	0,301	0,243	0,163	0,370	**0,823**	0,031
Aliphatics	**Aliphatics**	2874	0,362	0,278	0,260	0,438	**0,722**	0,025
	Aliphatics	2926	0,404	0,337	0,174	0,463	**0,661**	0,009
Phosphate/silicate signal	**Phosphates**	471	0,040	0,127	0,573	0,072	0,029	**0,796**

phosphate ions inhibits in vivo bioapatite crystal maturation. The presence of biogenic carbonates (i.e., molluscs shells) at the studied site [55], may have led to the incorporation of secondary carbonates in the bones and, therefore, creating a more stable bioapatite and an increased recrystallization rate [9,12]. This hypothesis is supported by the presence of a subtle band at 714 cm^{-1} in some of the samples that is most likely indicative of calcite precipitation [4,9,35,58,74,76,78]., Kontopoulos et al. [76] observed that crystal order increases with calcite uptake, since IRSF was higher in samples in which this calcite band was present. In our study the IRSF and the band at 714 cm^{-1} correlate negatively ($r_s = -0.633$; $p = <0.001$), indicating that changes in bioapatite crystallinity are not related to secondary carbonates. The IRSF values are within the range established by France et al. [17] for good bone preservation and agrees with the macroscopic study of the skeletons [49]. However, IRSF values are higher than those of reference for modern samples [24,74]. The negative correlation of IRSF with C/P suggest that the post-Roman skeletons from A Lanzada have been subjected to diagenetic alteration. This is consistent with research on chemical elemental composition of the studied bones, which also indicated bioapatite alteration [40]. Thus, both high IRSF values, and low carbonate-to-phosphate ratio values are indicative of bioapatite alteration by dissolution and recrystallisation [79] – the loss of carbonate ions enable the apatite crystals to grow and get more organized [18,26,63,69].

Our results support the recommendation made by Beasley et al. [10,14] about the usefulness of comparing IRSF and C/P to assess bone diagenetic processes. Here, correlating IRSF with the 714 cm^{-1} band also helped to refute possible alteration by secondary carbonates. Therefore, we advise to not only calculate the FTIR indices but examine the whole spectrum, to obtain a more accurate understanding of diagenesis of bone– as recommended by Leskovar et al. [36].

4.2. Bone organic components

Some authors have proposed the Am/P index as a good predictor of collagen content [28,77] Am/P values for A Lanzada samples (0.14 ± 0.05) are lower than those reported for modern human bone (0.29–0.35) [69] and consistent with values reported for archaeological human bone (0.08–0.52) [18,24,69]. Scaggion et al. [67] proposed values of Am/P higher than 0.1 to be indicative of good collagen quality and quantity. Taking this value as reference, the average collagen preservation of our samples is good; however, Scaggion et al. [67] employed a different FTIR technique (ATR) and may not be an appropriate reference for transmission FTIR. Furthermore, Am/P index as well as PC1 scores of the rib samples correlate with collagen yield ($r_s = 0.717$, $p = 0.003$; $r_s = 0.817$, $p = <0.001$), confirming a relationship between the relative amount of extracted collagen and the intensity of absorbance of the Amide I band relative to phosphate absorbance intensity. However, there was no significant correlation between Am/P and collagen %C, % N and C:N ($r_s = 0.46$, $p = 0.213$; $r_s = 0.417$, $p = 0.265$; $r_s = -0.458$, $p = 0.215$, respectively) (for more information on these parameters and diet reconstruction, see[80]). This indicates that Am/P and PC1 are more connected to bone collagen content than to collagen structural/compositional integrity.

PC3 also accounts for collagen content and denaturalization processes (amide III and the CH_2 wagging bands, located between 1400 and

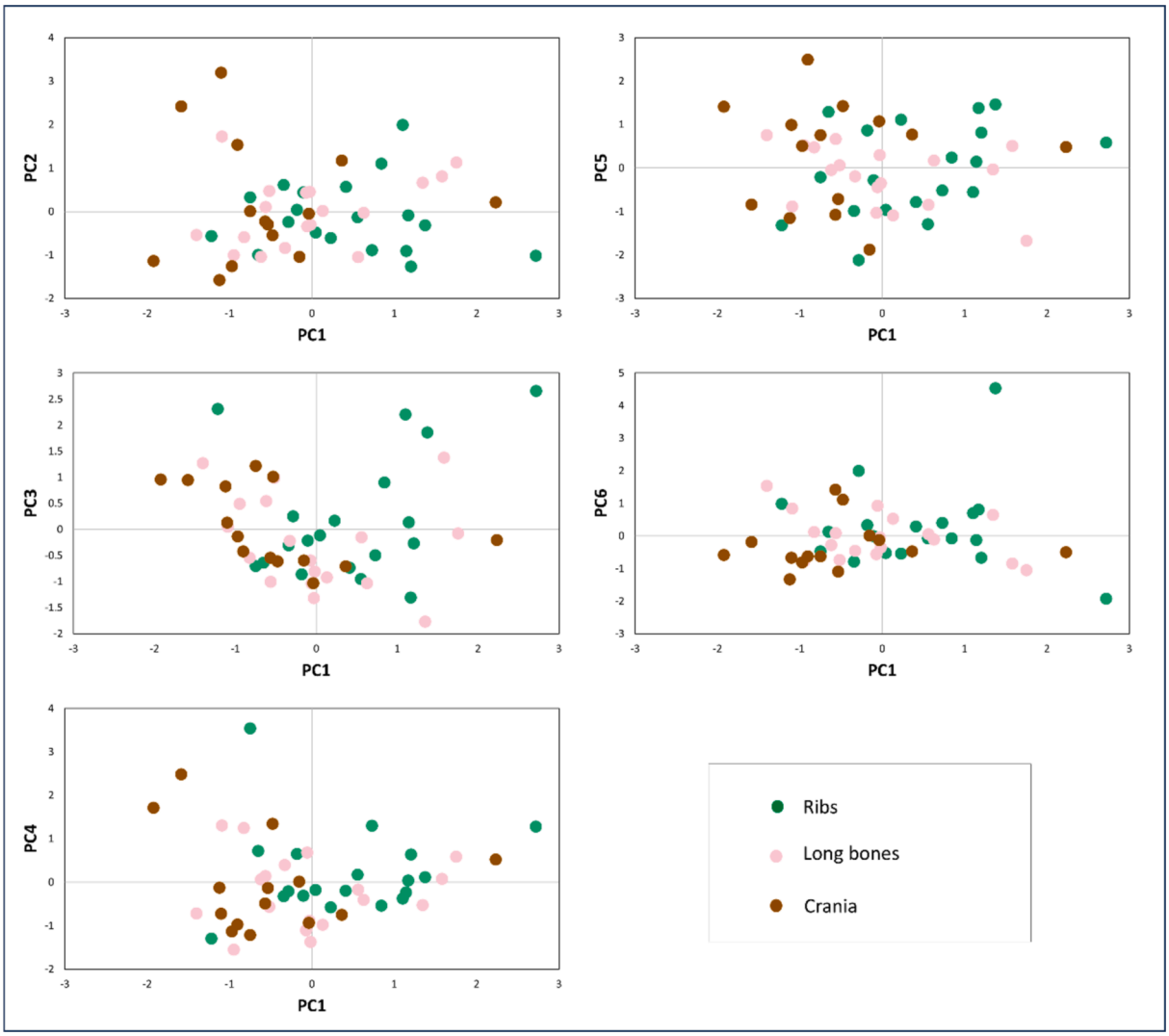

Fig. 4. Principal component scores for samples displayed in separate groups by bone type. Rib (green); long bone (brown); cranium (pink).

1100 cm^{-1} [81,82]). Amide III band is considered to be a good indicator of changes in collagen structure; while the CH_2 wagging band is indicative of collagen proline side chain [81] and changes in collagen structure (its intensity decreases with protein denaturalization). In our samples, Amide III bands are not grouped in the same PC as the other amide bands, meaning that these collagen bonds may have been altered in a different way – note that no difference according to bone type was found for PC3 scores. Similar results were found by Leskovar et al. [83] as they detected that absorbance in the Amide III region was higher for diaphysis compared with epiphysis in metacarpals and metatarsals, while Amide I absorbance was higher for epiphysis.

Collagen decays through bacterial attack and hydrolysis is assumed to be key in triggering bioapatite alteration and recrystallization [5,67,84]. In our samples, the relative collagen content (reflected by Am/P) is not correlated with the bioapatite crystallinity indicators (IRSF and MMI). This lack of correlation has been reported before [17,24,25,64,77,85] and attributed to differences in the rate of processes like dissolution, recrystallization and bioerosion [25]. Kontopoulos et al. [76] also suggested that bioapatite recrystallization can occur even if collagen content is high. In previous investigations in which we extracted collagen and bioapatite from the same bone sample, we observed that high-quality collagen is not indicative of good bioapatite preservation and the other way round [86,87]. Thereby, collagen quality indicators such as C:N, %C and %N, should not be used as indicators of bioapatite preservation and vice versa [10,17].

4.3. *Differences in bone type*

There are statistically significant differences in collagen content (PC1, Am/P) between ribs and crania, and between ribs and femur (Am/P), being higher in ribs. This is not surprising, since Álvarez-Fernández et al. [56] also identified significant differences in Am/P between bone types (rib/spine/ilium vs long bones/crania) for three post-Roman individuals excavated in 2016 in A Lanzada. This may imply structural pre-mortem differences in bone composition, in turnover rates, diagenesis, or a combination of both. Collagen content in human bone was found to be slightly higher in ribs than in femora and attributed to ante-mortem differences [88]. We did not find any in vivo data to interpret the observed differences between cranial bones, ribs, and femora. However, cranial bones are formed by intramembranous ossification, while ribs and femora are formed by endochondral ossification. Thus, ossification type and rates may play a role in the ante-mortem differences in bone collagen. Regarding in vivo turnover rates, ribs are assumed to have a slightly higher turnover rate [89] than other bones such as femora [90]. As far as we know, there are no specific data for turnover rates for crania, rather than the lack of bone turnover in petrous bone [91].

Regarding bone diagenesis, a previous study on bone elemental

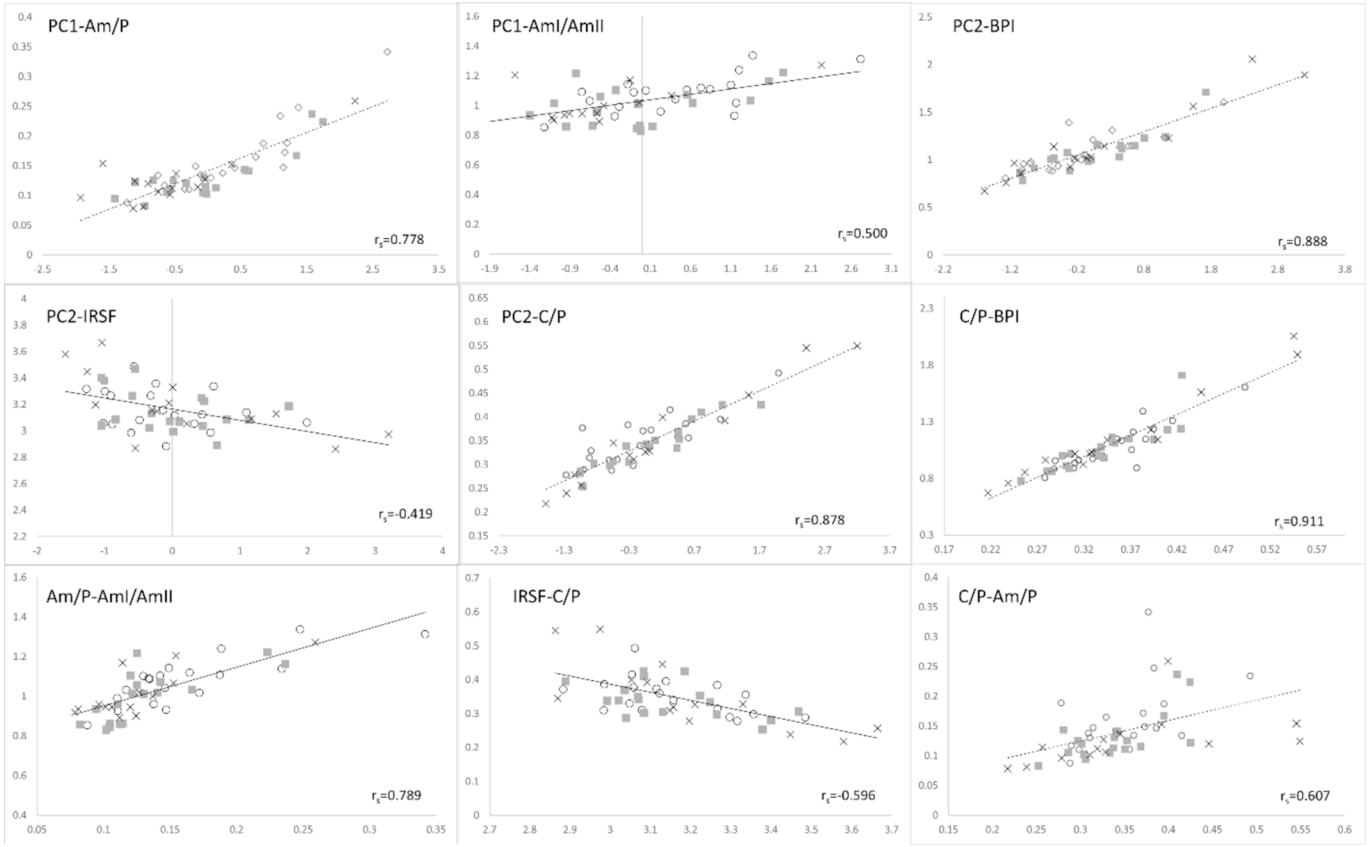

Fig. 5. Spearman correlation analysis between principal components and IR indices. Rib samples = circles; long bone samples = squares; crosses = cranium samples. PC1 = principal component 1; PC2 = principal component 2; Am/P = Amide I/phosphate; AmI/AmII = amide I/amide II; BPI = B-type carbonate/phosphate; IRSF = infrared splitting factor; C/P = carbonate/phosphate.

composition developed by our team [40] on skeletons from A Lanzada showed significant differences between ribs and the other two bone types considered. Ribs showed significant lower concentrations of bone constituent elements (Ca, P, Sr) but higher concentrations of chemical elements representative of soil contamination (Fe, Al, Si) and Ca/P values. The authors concluded that ribs were more prone to diagenesis than femora and cranial bones. Thus, the relatively higher content of collagen in ribs may be explained by a preferential loss of the inorganic component, i.e., the preferential alteration of bioapatite could have caused a relative (indirect) enrichment of collagen. In contrast, in a recent study on early bone diagenesis, Maurer et al. [25] detected lower and more heterogenous crystallinity in ribs than in femora and tibia and interpreted it as a better preservation of ribs in their collection. However, these authors [25] focussed their approach on mineralogy and molecular composition of collagen + bioapatite (FTIR/XRD) and, in our opinion, did not consider possible ante-mortem differences between bones (except for the differences in bone composition due to age-at-death).

Significantly higher values of C/C are displayed in A Lanzada cranial bones when compared with ribs, suggesting that the proportion of A-type carbonate versus B-type carbonate is higher in crania; the latter being the more abundant carbonate substitution [31] Three explanations are possible: i) first, pre-mortem A-type carbonate substitutions could have been higher in cranium than in ribs – although, data on fresh bone is not available as far as we are aware; ii) second, post-mortem differential precipitation of secondary carbonates in crania and ribs may have occurred, mainly because of the more porous nature of the ribs. France et al. [17] observed that secondary precipitation affects both carbonate substitutions (A-type and B-type carbonate); and iii) third, the occurrence of post-mortem differences in diagenetic carbonate substitution patterns between bone types. Leskovar et al. [36] found that the older the bone sample the lower the A-type carbonate content, due to incorporation of exogenous carbonate, carbonate reorganization, or by preferential elimination of A-type carbonate ions. Other authors suggest that B-type carbonate is more susceptible to substitution by exogenous phosphate and other ions [77]. Thereby, a higher C/C index may be interpreted as lower carbonate substitution and, therefore, better preserved bone, and thus carbonate in cranium is less altered than carbonate in ribs in the studied individuals, although the spectroscopic signal may be influenced by the lipidic content, which also absorbs in the B-type carbonate region [30].

A combination of ante-mortem features and bone diagenesis are the most likely explanation for the observed differences between bones. However, other aspects related to the burial environment should also be considered. For example, Dal Sasso et al. [9] suggested that intraskeletal differences in FTIR indices may be related with localised changes in burial conditions. This is consistent with what was found by Martínez Cortizas and López-Costas [16] for bone collagen. They analysed collagen from different archaeological sites from NW Spain, including A Lanzada, and found that collagen decays differently even at microscale within the same site. Gonçalves et al. [30] also found evidence of differences in FTIR indices depending on the bone, which they attributed to the different number of samples analysed for each bone type, although they did not discard different remodelling rates or structural changes as possible causes. Consequently, these authors advise to select the same bone type when comparing FTIR indices between individuals. Leskovar et al. [33] found not only differences in some FTIR indices depending on bone type but also on body region, with higher relative carbonate content in bones from upper limbs and torso. Thus, differences in bone chemistry may also be affected by body region.

4.4. Differences per age-at-death and sex

As for the age-at-death, the carbonate-to-phosphate indicators (C/P, BPI, PC2) for cranial bones are significantly higher in non-adults than in adults, but no difference regarding age was found for ribs or femora. In addition, PC2 scores of cranial bones are positive (i.e., higher carbonate content) in non-adult individuals and negative (i.e., higher phosphate content) in most adult individuals. These results agree with previous research which compare carbonate content in foetal and/or non-adult individuals versus that of adult individuals [3,25,92], changes (i.e., increase) in the BPI index with age [29], and changes (i.e., decrease) in the carbonate-to-phosphate ratio with age [93]. Other studies have reported opposite results. Caruso et al. [24] found higher carbonate content in adults than in non-adults and attributed it to an enrichment in carbonate in the bone mineral lattice during growth of the skeleton. Akkus et al. [94] found that C/P decreased until the mid-third decade, then increased until 44-year-old and remained unchanged for older individuals. Similar results were obtained by Yerramshety et al. [95], who observed an increase in B-type carbonate with age in cortical femoral bone of male individuals of 52–85 years old. Leskovar et al. [92] found that the relative carbonate content in tarsals was higher in old adults than in young and middle-aged adults. Considering the demographic profile of our collection (the adult group dominated by young adults), our study is consistent with a decrease in carbonate content during life, at least until young/middle age adulthood. Also, in our samples, C/P, BPI and PC2 for cranium are slightly higher in middle-aged adults and the old adult individual compared with the young adults. Thus, we hypothesize a non-linear trend in the change in bone carbonate content with age, with a general decrease until the fourth/fifth decade of life and an increase at greater age.

A possible explanation for the decrease in carbonate content may be the release of calcium carbonate to correct metabolic acidosis, which is known to increase with age [96]. Other alternatives are related to diagenesis: i) a differential incorporation of secondary carbonate ions (higher in bones from non-adult individuals), or ii) higher degradation of non-adult bones. In a previous soil study of two post-Roman burials from A Lanzada abundant primary carbonates (biogenic, i.e., shells) were found [55] and their chemical alteration may have released carbonate ions that could have been preferentially uptaken by the most porous bones of non-adults. Alternatively, non-adult skeletons are often reported as more susceptible to diagenesis than those of adults due to the poorly organized bone matrix, rich in collagen, and the highly porous mineral structure [24,26,35,97]. Differences in the histological structure in cortical bone between non-adult and adult individuals were also observed [24] and were related to different deterioration rates for skeletal tissues of juvenile and adult individuals.

We found no significant changes related to age-at-death in collagen content, Am/P or IRSF; and regarding sex, no FTIR index or PC showed significant differences between males and females, with the exception of PC2 for ribs. We interpret this later significance as a statistical bias, since they are likely related to two female samples with extremely high values. No significant correlations between collagen content (neither in spectroscopic signal neither in collagen C/N, %C, %N) and age-at-death were found. The lack of correlation may be due to the ante-mortem collagen content in bone, that is higher in non-adults, and for the A Lanzada individuals it may be hidden by a differential diagenetic alteration of collagen in non-adults, balancing the content and causing the lack of statistical differences. Despite our dataset being one of the largest generated up to now, the number of samples analysed here and in previous studies is still low and, when they are divided into groups can introduce biases in the interpretation due to the sample size effect.

5. Conclusions

The aim of this study was to infer ante-mortem differences and trace diagenetic changes in skeletons of the post-Roman population of A Lanzada archaeological site, paying special attention to bone type, sex and age-at-death. A Lanzada post-Roman individuals present a relatively low crystallinity index, which is negatively correlated with carbonate-to-phosphate index. Furthermore, the bones show a high carbonate content, probably due to secondary calcite precipitation, as a result of the weathering of the abundant biogenic carbonates in the soil of the site. Am/P is not correlated with IRSF, and the Amide III signal decays differently than that of Amide I, II, A and B in the A Lanzada samples. The lack of correlation was also observed in previous investigations and supports the hypothesis that collagen and bioapatite degradation are not as intertwined as previously thought. Bioapatite can be exposed to diagenesis regardless of collagen alteration and vice versa. Furthermore, the Am/P index shows a relationship between collagen and phosphate, but a high value for this index does not necessarily indicates good collagen preservation, but it may indicate that bioapatite is highly altered instead. Since this index is not correlated with collagen quality parameters (%N, %C, C/N), it may not be a good indicator to assess collagen preservation but only collagen relative content. Thus, the use of this index must be carefully considered. Statistical differences in PC1, Am/P and C/C between rib and cranium were found. Collagen relative content was higher in ribs and A-type carbonate relative to B-type carbonate was higher in cranium. No differences were observed between males and females. Furthermore, carbonate-to-phosphate ratio was significantly higher for non-adults than for adults, which may indicate a decrease of carbonate ions in bone with age, perhaps due to a metabolic mechanism to compensate (i.e., buffer) acidosis in older individuals. However, more studies with a statistically representative number of individuals of different age groups are needed to find out how the C/P changes with age-at-death. We highly recommend using the same bone type when possible. Notwithstanding these challenges FTIR is a useful tool to get insights into the ante-mortem chemical composition and post-mortem diagenetic alterations of different bone types. We advocate the adoption of a whole spectrum approach in future studies.

Funding sources

This project was funded by Grupos de Referencia Competitiva (ED431C 2021/32) by Xunta de Galicia and by the European Union (ERC Consolidator Grant, PollutedPast, 101087832). Views and opinions expressed are however those of the author(s) only and do not necessarily reflect those of the European Union or the European Research Council. Neither the European Union nor the granting authority can be held responsible for them. OLC is funded by Ramón y Cajal 2020 (RYC2020-030531-I) del Ministerio de Ciencia e Innovación. MCP is funded by Consolidación 2021 GRC GI-1553 – EcoPast. CVR is funded by predoctoral fellowship from Xunta de Galicia (ED481A 2022/205).

CRediT authorship contribution statement

Marta Colmenares-Prado: Formal analysis, Methodology, Writing – original draft, Visualization. **Antonio Martínez Cortizas:** Conceptualization, Data curation, Methodology, Supervision, Writing – original draft. **Clara Veiga-Rilo:** Formal analysis, Writing – original draft, Visualization. **Olalla López-Costas:** Conceptualization, Methodology, Supervision, Writing – original draft.

Declaration of competing interest

The authors declare the following financial interests/personal relationships which may be considered as potential competing interests: Antonio Martinez Cortizas reports financial support and article publishing charges were provided by Xunta de Galicia. Olalla Lopez-Costas reports financial support was provided by European Research Council. Olalla Lopez-Costas reports financial support was provided by Ministerio de Ciencia y Educacion, Gobierno de España. Clara Veiga-Rilo

reports financial support was provided by Xunta de Galicia. Marta Colmenares-Prado reports financial support was provided by Xunta de Galicia. If there are other authors, they declare that they have no known competing financial interests or personal relationships that could have appeared to influence the work reported in this paper.

Acknowledgements

We would like to thank the Museo Provincial de Pontevedra and the Dirección Xeral de Patrimonio of Xunta de Galicia for providing access to the skeletal collections. We would like to thank the RIAIDT-USC analytical facilities. We are grateful to thank Zaira García López for her help in map elaboration. We would like to express our gratitude to Bruker Optics for providing the image of the IFS 66V FTIR equipment, employed in the graphical abstract. We would like to thank Francisco Fariña for providing the image of the skeletons taken by him during the 1977 excavation of the site that has been used for the graphical abstract. We also want to thank Tim Mighall (Aberdeen University) for his comments and suggestions which helped to improve the manuscript.

Appendix A. Supplementary data

Supplementary data to this article can be found online at https://doi.org/10.1016/j.saa.2024.125675.

Data availability

Data will be made available on request.

References

[1] A.L. Boskey, P.G. Robey, The composition of bone, in: J.P. Bilezikian (Ed.), Primer on the Metabolic Bone Diseases and Disorders of Mineral Metabolism, Ninth Edition, John Wiley & Sons, 2019, pp. 84–92.
[2] A. El-Hussein, I. Yousef, M.A. Kasem, Exploiting FTIR microspectroscopy and chemometric analysis in the discrimination between Egyptian ancient bones: a case study, J. Opt. Soc. Am. B 37 (11) (2020) A110–A120, https://doi.org/10.1364/JOSAB.397419.
[3] B. Foley, M. Greiner, G. McGlynn, W.W. Schmahl, Anatomical variation of human bone bioapatite crystallography, Crystals 10 (10) (2020) 859, https://doi.org/10.3390/cryst10100859.
[4] F. Castorina, U. Masi, E. Giorgini, L. Mori, M.A. Tafuri, V. Notarstefano, Evidence for mild diagenesis in archaeological human bones from the Fewet necropolis (SW Libya): new insights and implications from ATR–FTIR spectroscopy, Appl. Sci. 13 (2) (2023) 687, https://doi.org/10.3390/app13020687.
[5] T. Tütken, T.W. Vennemann, Fossil bones and teeth: preservation or alteration of biogenic compositions? Palaeogeogr. Palaeoclimatol. Palaeoecol. 1 (310) (2011) 1–8, https://doi.org/10.1016/j.palaeo.2011.06.020.
[6] B. Cienkosz-Stepańczak, K. Szostek, A. Lisowska-Gaczorek, Optimizing FTIR method for characterizing diagenetic alteration of skeletal material, J. Archaeol. Sci. Rep. 38 (2021) 103059, https://doi.org/10.1016/j.jasrep.2021.103059.
[7] R.E. Hedges, Bone diagenesis: an overview of processes, Archaeometry 44 (3) (2002) 319–328, https://doi.org/10.1111/1475-4754.00064.
[8] C. Kendall, A.M.H. Eriksen, I. Kontopoulos, M.J. Collins, G. Turner-Walker, Diagenesis of archaeological bone and tooth, Palaeogeogr. Palaeoclimatol. Palaeoecol. 491 (2018) 21–37, https://doi.org/10.1016/j.palaeo.2017.11.041.
[9] G. Dal Sasso, M. Lebon, I. Angelini, L. Maritan, D. Usai, G. Artioli, Bone diagenesis variability among multiple burial phases at Al Khiday (Sudan) investigated by ATR-FTIR spectroscopy, Palaeogeogr. Palaeoclimatol. Palaeoecol. 463 (2016) 168–179, https://doi.org/10.1016/j.palaeo.2016.10.005.
[10] M.M. Beasley, M.J. Schoeninger, R. Miller, E.J. Bartelink, Preservation of bone organic fraction is not predictive of the preservation of bone inorganic fraction when assessing stable isotope analysis sample quality control measures, J. Archaeol. Sci. 162 (2024) 105886, https://doi.org/10.1016/j.jas.2023.105886.
[11] A. Person, H. Bocherens, J.F. Saliège, F. Paris, V. Zeitoun, M. Gérard, Early diagenetic evolution of bone phosphate: an X-ray diffractometry analysis, J. Archaeol. Sci. 22 (2) (1995) 211–221, https://doi.org/10.1006/jasc.1995.0023.
[12] F. Berna, A. Matthews, S. Weiner, Solubilities of bone mineral from archaeological sites: the recrystallization window, J. Archaeol. Sci. 31 (7) (2004) 867–882, https://doi.org/10.1016/j.jas.2003.12.003.
[13] P. Larkin, Infrared and Raman Spectroscopy: Principles and Spectral Interpretation, Elsevier, 2017.
[14] M.M. Beasley, E.J. Bartelink, L. Taylor, R.M. Miller, Comparison of transmission FTIR, ATR, and DRIFT spectra: implications for assessment of bone bioapatite diagenesis, J. Archaeol. Sci. 46 (2014) 16–22, https://doi.org/10.1016/j.jas.2014.03.008.
[15] M.M. Figueiredo, J.A.F. Gamelas, A.G. Martins, Characterization of bone and bone-based graft materials using FTIR spectroscopy, Infrared Spectrosc. Life Biomed. Sci. (2012) 315–338.
[16] A. Martínez Cortizas, O. López-Costas, Linking structural and compositional changes in archaeological human bone collagen: An FTIR-ATR approach, Sci. Rep. 10 (1) (2020) 17888, https://doi.org/10.1038/s41598-020-74993-y.
[17] C.A. France, N. Sugiyama, E. Aguayo, Establishing a preservation index for bone, dentin, and enamel bioapatite mineral using ATR-FTIR, J. Archaeol. Sci. Rep. 33 (2020) 102551, https://doi.org/10.1016/j.jasrep.2020.102551.
[18] H.I. Hollund, F. Ariese, R. Fernandes, M.M.E. Jans, H. Kars, Testing an alternative high-throughput tool for investigating bone diagenesis: FTIR in attenuated total reflection (ATR) mode, Archaeometry 55 (3) (2013) 507–532, https://doi.org/10.1111/j.1475-4754.2012.00695.x.
[19] C. Mircea, A. Vulpoi, I. Rusu, C. Radu, M. Pârvu, B. Kelemen, Exploring post-excavation degradation potential of fungal communities associated with archaeological human remains, Archaeometry 61 (3) (2019) 750–763, https://doi.org/10.1111/arcm.12438.
[20] R. Lindtner, A. Wurm, K. Kugel, J. Kühn, D. Putzer, R. Arora, D.C. Coraça-Huber, P. Zelger, M. Schirmer, J. Badzoka, C. Kappacher, C.W. Huck, J.D. Pallua, Comparison of mid-infrared handheld and benchtop spectrometers to detect Staphylococcus epidermidis in bone grafts, Bioengineering 10 (9) (2023) 1018, https://doi.org/10.3390/bioengineering10091018.
[21] C. Benetti, A. Blay, L. Correa, M.A. Verlangieri, M.O. Dos Santos, S.G. Kazarian, D. M. Zezell, ATR-FTIR spectroscopy imaging of bone repair in mandibular laser-osteotomy, J. Biophotonics (2024) e202400066, https://doi.org/10.1002/jbio.202400066.
[22] R. Chaber, C.J. Arthur, J. Depciuch, K. Łach, A. Raciborska, E. Michalak, J. Cebulski, Distinguishing Ewing sarcoma and osteomyelitis using FTIR spectroscopy, Sci. Rep. 8 (1) (2018) 15081, https://doi.org/10.1038/s41598-018-33470-3.
[23] S. Longato, C. Wöss, P. Hatzer-Grubwieser, C. Bauer, W. Parson, S.H. Unterberger, V. Kuhn, N. Pemberger, A.K. Pallua, W. Recheis, R. Lackner, R. Satlder, J.D. Pallua, Post-mortem interval estimation of human skeletal remains by micro-computed tomography, mid-infrared microscopic imaging and energy dispersive X-ray mapping, Anal. Methods 7 (7) (2015) 2917–2927, https://doi.org/10.1039/C4AY02943G.
[24] V. Caruso, N. Marinoni, V. Diella, E. Possenti, L. Mancini, M. Cantaluppi, F. Berna, C. Cattaneo, A. Pavese, Diagenesis of juvenile skeletal remains: a multimodal and multiscale approach to examine the post-mortem decay of children's bones, J. Archaeol. Sci. 135 (2021) 105477, https://doi.org/10.1016/j.jas.2021.105477.
[25] A.F. Maurer, V. Zeitoun, J. Bardin, A.R. Millard, L. Ségalen, F. Guérin, J.F. Saliège, A. Person, Multifactorial approach to describe early diagenesis of bones: the case study of the Merovingian cemetery of Saint-Linaire (France), Quat. Int. 660 (2023) 42–55, https://doi.org/10.1016/j.quaint.2023.03.003.
[26] H.L.Q. Stuart-Williams, H.P. Schwarcz, C.D. White, M.W. Spence, The isotopic composition and diagenesis of human bone from Teotihuacan and Oaxaca, Mexico, Palaeogeogr. Palaeoclimatol. Palaeoecol. 126 (1–2) (1996) 1–14, https://doi.org/10.1016/S0031-0182(96)00066-1.
[27] C.J. Yoder, E.J. Bartelink, Effects of different sample preparation methods on stable carbon and oxygen isotope values of bone apatite: a comparison of two treatment protocols, Archaeometry 52 (1) (2010) 115–130, https://doi.org/10.1111/j.1475-4754.2009.00473.x.
[28] M. Lebon, I. Reiche, X. Gallet, L. Bellot-Gurlet, A. Zazzo, Rapid quantification of bone collagen content by ATR-FTIR spectroscopy, Radiocarbon 58 (1) (2016) 131–145, https://doi.org/10.1017/RDC.2015.11.
[29] M. Pedrosa, F. Curate, L.A. Batista de Carvalho, M.P.M. Marques, M.T. Ferreira, Beyond metrics and morphology: the potential of FTIR-ATR and chemometrics to estimate age-at-death in human bone, Int. J. Leg. Med. 134 (5) (2020) 1905–1914, https://doi.org/10.1007/s00414-020-02310-3.
[30] D. Gonçalves, A.R. Vassalo, A.P. Mamede, C. Makhoul, G. Piga, E. Cunha, M.P. M. Marques, L.A. Batista de Carvalho, Crystal clear: Vibrational spectroscopy reveals intrabone, intraskeleton, and interskeleton variation in human bones, Am. J. Phys. Anthropol. 166 (2) (2018) 296–312, https://doi.org/10.1002/ajpa.23430.
[31] T. Leskovar, I. Zupanič Pajnič, I. Jerman, M. Črešnar, Preservation state assessment and post-mortem interval estimation of human skeletal remains using ATR-FTIR spectra, Aust. J. Forensic Sci. 54 (4) (2020) 511–532, https://doi.org/10.1080/00450618.2020.1836254.
[32] I. Zupanič Pajnič, T. Leskovar, I. Jerman, ATR-FTIR spectroscopy and chemometric complexity: unfolding the intra-skeleton variability, J. Chemom. 36 (11) (2022) e3448, https://doi.org/10.1002/cem.3448.
[33] T. Leskovar, I. Zupanič Pajnič, I. Jerman, Dealing with minor differences in bone matrix: can spectra follow the DNA preservation? Aust. J. Forensic Sci. 55 (2) (2023) 203–222, https://doi.org/10.1080/00450618.2021.1948102.
[34] C.M. Nielsen-Marsh, C.I. Smith, M.M. Jans, A. Nord, H. Kars, M.J. Collins, Bone diagenesis in the European Holocene II: taphonomic and environmental considerations, J. Archaeol. Sci. 34 (9) (2007) 1523–1531, https://doi.org/10.1016/j.jas.2006.11.012.
[35] S.H. Bayarı, K. Özdemir, E.H. Sen, C. Araujo-Andrade, Y.S. Erdal, Application of ATR-FTIR spectroscopy and chemometrics for the discrimination of human bone remains from different archaeological sites in Turkey, Spectrochim. Acta A Mol. Biomol. Spectrosc. 237 (2020) 118311, https://doi.org/10.1016/j.saa.2020.118311.
[36] T. Leskovar, I. Zupanič Pajnič, I. Jerman, M. Črešnar, Separating forensic, WWII, and archaeological human skeletal remains using ATR-FTIR spectra, Int. J. Leg. Med. 134 (2020) 811–821, https://doi.org/10.1007/s00414-019-02079-0.

[37] A.L. Boskey, E. DiCarlo, E. Paschalis, P. West, R. Mendelsohn, Comparison of mineral quality and quantity in iliac crest biopsies from high-and low-turnover osteoporosis: an FT-IR microspectroscopic investigation, Osteoporos. Int. 16 (2005) 2031–2038, https://doi.org/10.1007/s00198-005-1992-3.
[38] H.H. Malluche, D.S. Porter, M.C. Monier-Faugere, H. Mawad, D. Pienkowski, Differences in bone quality in low-and high-turnover renal osteodystrophy, J. Am. Soc. Nephrol. 23 (3) (2012) 525–532, https://doi.org/10.1681/ASN.2010121253.
[39] A. El-Husseini, M. Abdalbary, F. Lima, M. Issa, M.T. Ahmed, M. Winkler, H. Srour, D. Davenport, G. Wang, M.C. Faugere, H.H. Malluche, Low turnover renal osteodystrophy with abnormal bone quality and vascular calcification in patients with mild-to-moderate CKD, Kidney Int. Rep. 7 (5) (2022) 1016–1026, https://doi.org/10.1016/j.ekir.2022.02.022.
[40] O. López-Costas, O. Lantes-Suarez, A.M. Cortizas, Chemical compositional changes in archaeological human bones due to diagenesis: Type of bone vs soil environment, J. Archaeol. Sci. 67 (2016) 43–51, https://doi.org/10.1016/j.jas.2016.02.001.
[41] O. López-Costas, G. Müldner, Fringes of the empire: Diet and cultural change at the Roman to post-Roman transition in NW Iberia, Am. J. Phys. Anthropol. 161 (1) (2016) 141–154, https://doi.org/10.1002/ajpa.23016.
[42] A. Blanco Freijeiro, M.E. Fusté Ara, A. Garcia Alen, La necrópolis galaico-romana de La Lanzada (Noalla, Pontevedra), I, Cuadernos De Estudios Gallegos 16 (1961) 141–158.
[43] A. Blanco Freijeiro, M.E. Fusté Ara, A. Garcia Alen, La necrópolis galaico-romana de La Lanzada (Noalla, Pontevedra), II, Cuadernos De Estudios Gallegos 22 (5–23) (1967) 129–155.
[44] F. Busto, Excavación de A Lanzada (Sanxenxo-Pontevedra); Informe preliminar de la campaña, Museo De Pontevedra 29 (1975) 165–173.
[45] F. Fariña Busto, J.E. Filgueira Valverde, Plan Nacional de Excavaciones 1973: A Lanzada (Sanjenjo, Pontevedra), Museo De Pontevedra 28 (1974) 83–86.
[46] A. Peña Santos, A Lanzada (excavación de urgencia en 1981), Museo De Pontevedra 36 (1982) 77–78.
[47] R.M. Rodríguez Martínez, Intervención arqueolóxica para a recuperación patrimonial do xacemento de A Lanzada (Sanxenxo, Pontevedra). Informe valorativo, in: Original Depositado En Consellería De Cultura e Deporte. Dirección Xeral De Patrimonio. Xunta De Galicia, 2010, p. 49.
[48] R.M. Rodríguez Martínez, R. Aboal Fernandez, V. Castro Hierro, C. Candela Cereijo, J.M. Ayán Vila, Una posible factoría prerromana en el noroeste. Primeras valoraciones de la intervención en el Campo de A Lanzada (Sanxenxo, Pontevedra), Férvedes 7 (2011) 159–168.
[49] O. Lopez-Costas, Taphonomy and burial context of the Roman/post-Roman funerary areas (2nd to 6th centuries AD) of A Lanzada, NW Spain, Estudos Do Quaternario/quaternary Studies 12 (2015) 55–67, https://doi.org/10.30893/eq.v0i12.111.
[50] O. López-Costas, Antropología de los restos óseos humanos de Galicia: estudio de la población romano y medieval gallega, Universidad de Granada, Granada, 2012, p. 555.
[51] O. López-Costas, M. Kylander, N. Mattielli, N. Álvarez-Fernández, M. Pérez-Rodríguez, T. Mighall, R. Bindler, C.A. Martínez, Human bones tell the story of atmospheric mercury and lead exposure at the edge of Roman World, Sci. Total Environ. 710 (2020) 136319, https://doi.org/10.1016/j.scitotenv.2019.136319.
[52] N. Álvarez-Fernández, A.M. Cortizas, O. López-Costas, Atmospheric mercury pollution deciphered through archaeological bones, J. Archaeol. Sci. 119 (2020) 105159, https://doi.org/10.1016/j.jas.2020.105159.
[53] K. Squires, T. Booth, C.A. Roberts, The ethics of sampling human skeletal remains for destructive analyses, Ethical Approaches to Human Remains: A Global Challenge in Bioarchaeology and Forensic Anthropology 265–297 (2019), https://doi.org/10.1007/978-3-030-32926-6_12.
[54] H.V. Vallois, Vital statistics in prehistoric populations as determined from archaeological data, The Application of Quantitative Methods in Archaeology 28 (1960) 186.
[55] Z. García-López, A. Martínez Cortizas, N. Álvarez-Fernández, O. López-Costas, Understanding Necrosol pedogenetical processes in post-Roman burials developed on dunes sands, Sci. Rep. 12 (1) (2022) 10619, https://doi.org/10.1038/s41598-022-14750-5.
[56] N. Álvarez-Fernández, A.M. Cortizas, O. López-Costas, Structural equation modelling of mercury intra-skeletal variability on archaeological human remains, Sci. Total Environ. 851 (2022) 158015, https://doi.org/10.1016/j.scitotenv.2022.158015.
[57] N. Álvarez Fernández, A. Martínez Cortizas, andurinha: Make Spectroscopic Data Proccessing Easier. (2020).
[58] A. Grunenwald, C. Keyser, A.M. Sautereau, E. Crubézy, B. Ludes, C. Drouet, Revisiting carbonate quantification in apatite (bio) minerals: a validated FTIR methodology, J. Archaeol. Sci. 49 (2014) 134–141, https://doi.org/10.1016/j.jas.2014.05.004.
[59] A.P. Mamede, D. Gonçalves, M.P.M. Marques, L.A. Batista de Carvalho, Burned bones tell their own stories: A review of methodological approaches to assess heat-induced diagenesis, Appl. Spectrosc. Rev. 53 (8) (2018) 603–635, https://doi.org/10.1080/05704928.2017.1400442.
[60] E.A. Taylor, E. Donnelly, Raman and Fourier transform infrared imaging for characterization of bone material properties, Bone 139 (2020) 115490, https://doi.org/10.1016/j.bone.2020.115490.
[61] N. Kourkoumelis, X. Zhang, Z. Lin, J. Wang, Fourier transform infrared spectroscopy of bone tissue: bone quality assessment in preclinical and clinical applications of osteoporosis and fragility fracture, Clin. Rev. Bone Miner. Metab. 17 (2019) 24–39, https://doi.org/10.1007/s12018-018-9255-y.
[62] K.H. Liland, B.H. Mevik, R. Canteri, Baseline correction of spectra. R Package version 1.3-4 (2020).
[63] D.R. Smith, E.K. Martin, B.L. Kaufman, M. Callaghan, K. Cardona, B. Kovacevich, J. M. Toyne, The bottom line: Exploring analytical methods for assessing bioapatite preservation in archaeological bone using FTIR-ATR, J. Archaeol. Sci. Rep. 50 (2023) 104014, https://doi.org/10.1016/j.jasrep.2023.104014.
[64] S. Weiner, O. Bar-Yosef, States of preservation of bones from prehistoric sites in the Near East: a survey, J. Archaeol. Sci. 17 (2) (1990) 187–196, https://doi.org/10.1016/0305-4403(90)90058-D.
[65] D. Farlay, G. Panczer, C. Rey, P.D. Delmas, G. Boivin, Mineral maturity and crystallinity index are distinct characteristics of bone mineral, J. Bone Miner. Metab. 28 (2010) 433–445, https://doi.org/10.1007/s00774-009-0146-7.
[66] C.N. Trueman, A.K. Behrensmeyer, N. Tuross, S. Weiner, Mineralogical and compositional changes in bones exposed on soil surfaces in Amboseli National Park, Kenya: diagenetic mechanisms and the role of sediment pore fluids, J. Archaeol. Sci. 31 (6) (2004) 721–739, https://doi.org/10.1016/j.jas.2003.11.003.
[67] C. Scaggion, G. Dal Sasso, L. Nodari, L. Pagani, N. Carrara, A. Zotti, T. Banzato, D. Usai, L. Pasqualetto, G. Gadioli, G. Artioli, An FTIR-based model for the diagenetic alteration of archaeological bones, J. Archaeol. Sci. 161 (2024) 105900, https://doi.org/10.1016/j.jas.2023.105900.
[68] L.U.T.Z. Nasdala, D.C. Smith, R. Kaindl, M.A. Ziemann, Raman spectroscopy: analytical perspectives in mineralogical research. (2004).
[69] A. Grunenwald, C. Keyser, A.M. Sautereau, E. Crubézy, B. Ludes, C. Drouet, Novel contribution on the diagenetic physicochemical features of bone and teeth minerals, as substrates for ancient DNA typing, Anal. Bioanal. Chem. 406 (2014) 4691–4704, https://doi.org/10.1007/s00216-014-7863-z.
[70] T.J.U. Thompson, M. Gauthier, M. Islam, The application of a new method of Fourier Transform Infrared Spectroscopy to the analysis of burned bone, J. Archaeol. Sci. 36 (3) (2009) 910–914, https://doi.org/10.1016/j.jas.2008.11.013.
[71] R. Fernandes, M. Sponheimer, P. Roberts, TOOTHFIR: Presenting a dataset and a preliminary meta-analysis of Fourier Transform Infra-red Spectroscopy indices from archaeological and palaeontological tooth enamel, Quat. Int. 650 (2023) 77–85, https://doi.org/10.1016/j.quaint.2022.01.010.
[72] A. Adamiano, D. Fabbri, G. Falini, M.G. Belcastro, A complementary approach using analytical pyrolysis to evaluate collagen degradation and mineral fossilisation in archaeological bones: The case study of Vicenne-Campochiaro necropolis (Italy), J. Anal. Appl. Pyrol. 100 (2013) 173–180, https://doi.org/10.1016/j.jaap.2012.12.014.
[73] A.Y.A. Dalou, A.M. ElSerogy, A.A. Al-Shorman, M. Alrousan, A. Khwaileh, Bioarchaeology, conservation and display of a 16k-human skeleton, Jordan, Medit. Archaeol. Archaeom. 17 (1) (2017) 251–263, https://doi.org/10.5281/zenodo.400781.
[74] L.E. Wright, H.P. Schwarcz, Infrared and isotopic evidence for diagenesis of bone apatite at Dos Pilas, Guatemala: palaeodietary implications, J. Archaeol. Sci. 23 (6) (1996) 933–944, https://doi.org/10.1006/jasc.1996.0087.
[75] J.Z. Metcalfe, F.J. Longstaffe, C.D. White, Method-dependent variations in stable isotope results for structural carbonate in bone bioapatite, J. Archaeol. Sci. 36 (1) (2009) 110–121, https://doi.org/10.1016/j.jas.2008.07.019.
[76] I. Kontopoulos, K. Penkman, I. Liritzis, M.J. Collins, Bone diagenesis in a Mycenaean secondary burial (Kastrouli, Greece), Archaeol. Anthropol. Sci. 11 (2019) 5213–5230, https://doi.org/10.1007/s12520-019-00853-0.
[77] I. Kontopoulos, K. Penkman, G.D. McAllister, N. Lynnerup, P.B. Damgaard, H. B. Hansen, M.E. Allentoft, M.J. Collins, Petrous bone diagenesis: a multi-analytical approach, Palaeogeogr. Palaeoclimatol. Palaeoecol. 518 (2019) 143–154, https://doi.org/10.1016/j.palaeo.2019.01.005.
[78] J.A. Lee-Thorp, N.J. Van der Merwe, Aspects of the chemistry of modern and fossil biological apatites, J. Archaeol. Sci. 18 (3) (1991) 343–354, https://doi.org/10.1016/0305-4403(91)90070-6.
[79] C.L. King, N. Tayles, K.C. Gordon, Re-examining the chemical evaluation of diagenesis in human bone apatite, J. Archaeol. Sci. 38 (9) (2011) 2222–2230, https://doi.org/10.1016/j.jas.2011.03.023.
[80] G.J. Van Klinken, Bone collagen quality indicators for palaeodietary and radiocarbon measurements, J. Archaeol. Sci. 26 (6) (1999) 687–695, https://doi.org/10.1006/jasc.1998.0385.
[81] M. Jackson, P.H. Watson, W.C. Halliday, H.H. Mantsch, Beware of connective tissue proteins: assignment and implications of collagen absorptions in infrared spectra of human tissues, Biochim. Biophys. Acta (BBA)-Mol. Basis Dis. 1270 (1) (1995) 1–6, https://doi.org/10.1016/0925-4439(94)00056-V.
[82] M.A. Kasem, I. Yousef, Z.A. Alrowaili, M. Zedan, A. El-Hussein, Investigating Egyptian archeological bone diagenesis using ATR-FTIR microspectroscopy, J. Radiat. Res. Appl. Sci. 13 (1) (2020) 515–527, https://doi.org/10.1080/16878507.2020.1752480.
[83] T. Leskovar, J. Inkret, I. Zupanič Pajnič, I. Jerman, Comparison of DNA preservation and ATR-FTIR spectroscopy indices of cortical and trabecular bone of metacarpals and metatarsals, Sci. Rep. 13 (1) (2023) 15498, https://doi.org/10.1038/s41598-023-41259-2.
[84] G. Gallo, M. Fyhrie, C. Paine, S.V. Ushakov, M. Izuho, B. Gunchinsuren, N. Zwyns, A. Navrotsky, Characterization of structural changes in modern and archaeological burnt bone: implications for differential preservation bias, PLoS One 16 (7) (2021) e0254529, https://doi.org/10.1371/journal.pone.0254529.
[85] M. Lebon, I. Reiche, J.J. Bahain, C. Chadefaux, A.M. Moigne, F. Fröhlich, F. Sémah, H.P. Schwarcz, C. Falguéres, New parameters for the characterization of diagenetic alterations and heat-induced changes of fossil bone mineral using Fourier

transform infrared spectrometry, J. Archaeol. Sci. 37 (9) (2010) 2265–2276, https://doi.org/10.1016/j.jas.2010.03.024.
[86] O. López-Costas, G. Müldner, Boom and bust at a medieval fishing port: dietary preferences of fishers and artisan families from Pontevedra (Galicia, NW Spain) during the Late Medieval and Early Modern Period, Archaeol. Anthropol. Sci. 11 (2019) 3717–3731, https://doi.org/10.1007/s12520-018-0733-4.
[87] C. Veiga-Rilo, A.M. Cortizas, O. López-Costas, Biting into the truth: Connecting oral pathology and stable isotopes through the paradigmatic example of a hyper-specialized marine diet in Medieval Pontevedra (NW Iberia), Archaeol. Anthropol. Sci. 16 (4) (2024) 49, https://doi.org/10.1007/s12520-024-01956-z.
[88] J.-M. Mbuyi-Muamba, J. Dequeker, Biochemical anatomy of human bone: comparative study of compact and spongy bone in femur, rib and iliac crest, Acta Anat. 128 (3) (1987) 184–187, https://doi.org/10.1159/000146337.
[89] R.L. Quinn, How much time is recorded with a rib bone isotope? J. Archaeol. Sci. Rep. 57 (2024) 104593 https://doi.org/10.1016/j.jasrep.2024.104593.
[90] R.E. Hedges, J.G. Clement, C.D.L. Thomas, T.C. O'connell, Collagen turnover in the adult femoral mid-shaft: Modeled from anthropogenic radiocarbon tracer measurements, Am. J. Phys. Anthropol. 133 (2) (2007) 808–816, https://doi.org/10.1002/ajpa.20598.
[91] M.L.S. Jørkov, J. Heinemeier, N. Lynnerup, The petrous bone—A new sampling site for identifying early dietary patterns in stable isotopic studies, Am. J. Phys. Anthropol. 138 (2) (2009) 199–209, https://doi.org/10.1002/ajpa.20919.
[92] T. Leskovar, I. Jerman, I.Z. Pajnič, Unveiling intra-skeletal variability in mature and immature human skeletal remains via ATR-FTIR spectroscopy, Vib. Spectrosc 132 (2024) 103688, https://doi.org/10.1016/j.vibspec.2024.103688.
[93] E.P. Paschalis, E. DiCarlo, F. Betts, P. Sherman, R. Mendelsohn, A.L. Boskey, FTIR microspectroscopic analysis of human osteonal bone, Calcif. Tissue Int. 59 (1996) 480–487, https://doi.org/10.1007/BF00369214.
[94] O. Akkus, A. Polyakova-Akkus, F. Adar, M.B. Schaffler, Aging of microstructural compartments in human compact bone, J. Bone Miner. Res. 18 (6) (2003) 1012–1019, https://doi.org/10.1359/jbmr.2003.18.6.1012.
[95] J.S. Yerramshetty, C. Lind, O. Akkus, The compositional and physicochemical homogeneity of male femoral cortex increases after the sixth decade, Bone 39 (6) (2006) 1236–1243, https://doi.org/10.1016/j.bone.2006.06.002.
[96] D.A. Bushinsky, Acid-base imbalance and the skeleton, Eur. J. Nutr. 40 (2001) 238–244, https://doi.org/10.1007/s394-001-8351-5.
[97] J.D. Currey, G. Butler, The mechanical properties of bone tissue in children, J. Bone Joint Surg. 57 (6) (1975) 810–814.